Chitosan-pectin multilayer coating with anthocyanin grape dye as pH indicating wound dressing: Synthesis and characterization

Jovana Petkovska [a], Nikola Geskovski [b], Darka Marković [c], Vesna Dimova [a], Dejan Mirakovski [d], Maja Radetić [e], Igor Jordanov [a,*]

[a] Faculty of Technology and Metallurgy, Ss. Cyril and Methodius University in Skopje, Ruger Boskovic 16, Skopje 1000, North Macedonia
[b] Institute of Pharmaceutical Technology, Faculty of Pharmacy, University of Ss. Cyril and Methodius in Skopje, Majka Tereza 47, Skopje 1000, North Macedonia
[c] Innovation Centre of the Faculty of Technology and Metallurgy, University of Belgrade, Karnegijeva 4, Belgrade 11120, Serbia
[d] Faculty of Natural and Technical Science, Goce Delcev University, Krste Misirkov 10-A, Shtip 2000, North Macedonia
[e] Faculty of Technology and Metallurgy, University of Belgrade, Karnegijeva 4, Belgrade 11120, Serbia

ARTICLE INFO

ABSTRACT

Environmentally benign pH-indicating wound dressing comprised of carbohydrates chitosan (CH) and pectin (P), and anthocyanin grape (AG) dye is created via layer-by-layer assembly. Cotton fabric coated with eight bilayers of $(CH-AG)_4/(P-AG)_4$ deposited 1.97 % AG-dye. It exhibited a visible and immediate color change from pink to violet-blue while increasing its pH value from 6 to pH 7, matching the turning pH point of healing into an infected wound. Color transition of AG-dye in water-based buffers, tested by VIS-spectroscopy, shows the same color change when the pH value increased from 6 to 7. This coating imparts excellent antimicrobial activity against Gram-positive bacteria Staphylococcus aureus and yeast *Candida* albicans, moderate antibacterial activity against Gram-negative Escherichia coli bacteria, and no cytotoxicity on human fibroblast cells (MRC-5). This research proposes a sustainable, low-cost, and simple method for obtaining smart wound dressing that provides real-time monitoring of the wound pH.

1. Introduction

Wound infection is the most common and dangerous complication that disrupts and prolongs wound healing and could lead to sepsis or, eventually, amputations of some parts of the human body (Pang et al., 2023). Detection of wound infection in a very early stage is crucial for appropriate wound treatment and healing. Wound dressing that gives visual (with the naked eye) information to healthcare staff on how the wound is evolving the future of wound dressings. Many factors influence wound infection, but the most common is the presence of bacterial and fungal microorganisms (Bowler et al., 2001). Since bacterial growth causes necrosis, the main reason for wound alkalization, the pH of the wound is considered an indicator of some infection (Bennison et al., 2020). A healthy wound typically has a pH value of around 4 to 6, while infected or compromised shows pH values above 7 (Gamerith et al., 2019). There are several materials for measuring the wound pH. Hydrogel-based passive wireless sensor (Sridhar & Takahata, 2009), pH and reference electrodes fabricated on a paper substrate (Rahimi et al., 2016), cotton swabs (Schaude et al., 2017), bandages (Kassal et al.,

2017; Mariani et al., 2021; Pal et al., 2018), pH sensor with near-field communication (Rahimi et al., 2018), and composite dressing (Nischwitz et al., 2019) are only some recently developed solutions. Although effective, these materials are expensive, need the intricate development of the instrument (tool/gadget), use synthetic dyes, do not have antimicrobial properties, require a prolonged time to measure the pH value of the wound, and can detect pH value only by taking a sample from the wound without being put directly on the wound.

The textile materials that employ indicator dyes to produce pH-indicating wound dressing are the most promising. Textile fabrics, with their light wear, elastic and breathable properties, are an ideal carrier for pH-indicating dyes, creating wound dressing that timely detects the change in the wound pH in constant direct contact with the wound (Derakhshandeh et al., 2018). Even promising, synthetic dye-containing wound dressings show serious drawbacks because they could be allergenic and cytotoxic (Yadav et al., 2023b). The modern pH-indicating wound dressing has to be made of natural, bio-sourced, non-allergenic, and non-cytotoxic chemistry that detects a change in pH in seconds (Pal et al., 2018). In recent years, there has been a

---

* Corresponding author.
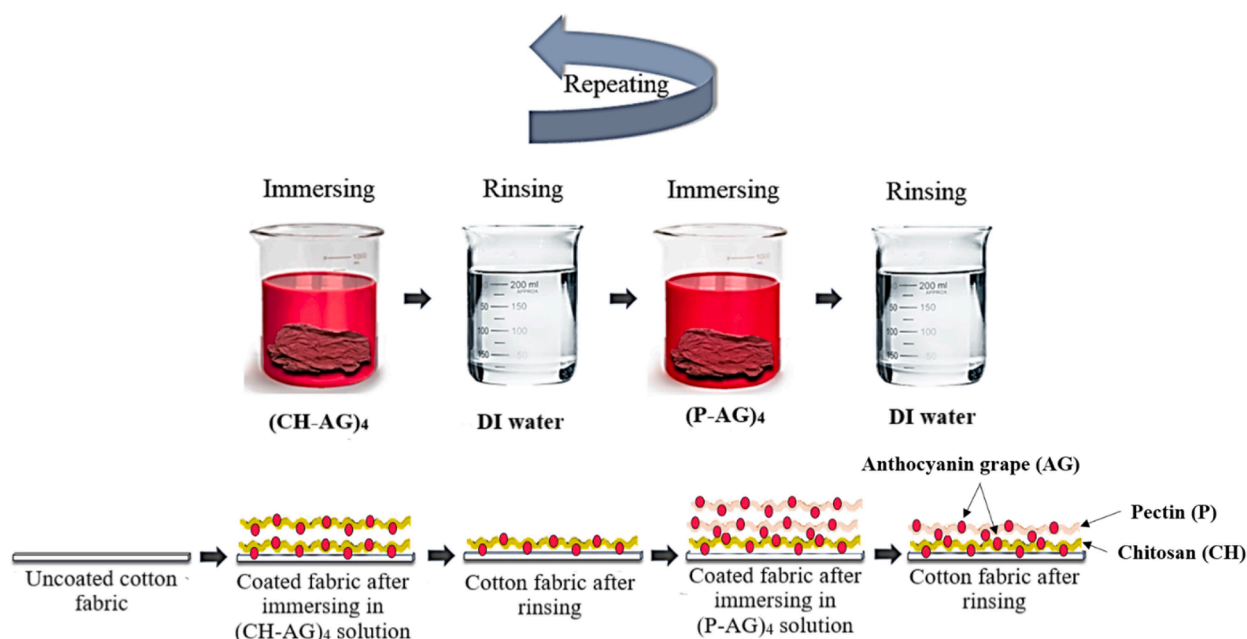*E-mail address:* jordanov@tmf.ukim.edu.mk (I. Jordanov).

Fig. 1. Schematic of LbL deposition.

growing interest in utilizing biopolymers such as chitosan (Yadav et al., 2023a), alginate (Singh et al., 2021), pectin (Sutar et al., 2021), gelatin (Karydis-Messinis et al., 2023), arginine and curcumin (Jian et al., 2023), and quercetin (Li et al., 2022), for the development of biomaterial-based anti-infecting wound dressings. These biopolymers combined with natural dyes as pH sensors, are the main components in modern pH-indicating wound dressings (Rani Raju et al., 2022). Anthocyanins, a class of natural dyes, are eco-friendly, water-soluble pigments that change color when exposed to acidic or alkaline medium (Mary et al., 2022; Yuan et al., 2023). Apart from being pH-sensitive, these pigments also demonstrate antibacterial and antifungal properties, very important features for wound healing. Recently, these pigments were employed as pH indicators in calcium alginate fiber (Cui et al., 2020), nanofibrous and alginate-based pH-sensing electrospun wound dressings (Pakolpakçıl et al., 2021), chitosan and cellulose-based hydrogels (Arafa et al., 2021), and filter paper (Kiti et al., 2022). Since anthocyanins are natural pigments that do not possess functional groups for creating strong bonds with the textile fibers, the main challenge in their application to the textile wound dressing is the dyeing of the textile fabrics with them. There are many attempts to dye cotton fabric with natural dye using mordants (Yadav et al., 2023b), but many of them have not achieved the desired color of the fabric and/or are toxic and non-ecofriendly (Saxena & Raja, 2014).

The Layer-by-Layer (LbL) assembly (Jordanov et al., 2020, 2019a, 2019b) is a relatively new technique that can be used for the successful dyeing of the cotton carrier (Khan et al., 2016) because this highly tailorable coating technique is an evolution of the nano-layer adsorption process. It is a simple, inexpensive, and environmentally friendly technique, performed through alternate immersion of the textile substrate in oppositely charged polyelectrolyte solutions, which pile up on the substrate surface, giving rise to a positively/negatively charged multilayer. This technique is successfully used for dyeing (Uğur & Sarıışık, 2011) and finishing textile materials (Magovac et al., 2020, 2021, 2022a, 2022b; Marković et al., 2023). Chitosan and pectin have been successfully applied via LbL assembly on polyester fabric to yield a flame retardant fabric (Petkovska et al., 2023). As mentioned before, chitosan and pectin are recognized for their anti-infecting properties in wound dressings. Therefore, in this research, chitosan-anthocyanin was paired with pectin-anthocyanin and was successfully applied on the surface of the cotton fabric to produce environmentally-benign pH-indicating

wound dressing from bio-sourced carbohydrates. Only 8 bilayers (BL) of this system firmly bonded a significant amount of anthocyanin grape dye, creating an intensively colored wound dressing capable of immediate pH assessment. Since all used chemicals are bio-sourced, this pH-indicating wound dressing shows no cytotoxicity on human fibroblast cells (MRC-5) while providing sufficiently high antibacterial and antifungal activity. The novelty of this research lies in creating pH-indicating wound dressing from bio-sourced polyelectrolytes and natural dye applied to the textile material as a carrier with a flexible and breathable structure. The porous LbL network of polyelectrolytes enables a quick response to pH change in a second, which is crucial in wound healing.

2. Materials and methods

2.1. Materials and chemicals

Bleached cotton fabric with a 135 g/m², 24 threads per cm warp density, and 20 threads per cm weft density was purchased from Alkaloid AD Berovo, North Macedonia. Anthocyanin grape (AG) dye was supplied from GNT (Mierlo, Netherlands), chitosan, with a molecular weight of 190,000–310,000 g/mol and degree of deacetylation (DD) of 75–85 %, was purchased from Carbosynth Limited (Compton, Berkshire, UK), and GRINDSTED pectin LC 810 was supplied from P.I.C. Co. DOOEL (Skopje, North Macedonia). Hydrochloric acid 37 % (HCl) and sodium hydroxide (NaOH) were purchased from Sigma-Aldrich. Sodium acetate, borax, and boric acid were provided by Alkaloid-Skopje (North Macedonia). Acetic acid was supplied by CARLO ERBA Reagents (France) while glycine was purchased from MERCK (Germany). Monopotassium phosphate was purchased from Riedel-de Haën AG Seelze-Hannover (Germany). All chemicals were used as received. All of the aqueous solutions were made with 18.2 MΩ deionized (DI) water at room temperature (21 °C ± 1 °C).

2.2. Methods

2.2.1. Preparation of solutions for LbL deposition

The positively charged chitosan (CH) solution was done by slowly adding and mixing 0.5 wt% chitosan in water with a pH of 1.7, adjusted by concentrated HCl. When the CH was completely dissolved, the pH of

the solution was adjusted to 4 with 1 M and 0.1 M NaOH. A negatively charged 0.5 wt% water-based pectin (P) solution was obtained by dissolving a defined amount of pectin into DI water and mixing until a homogenous solution was obtained. The pH of the solution was adjusted to 4 using 0.1 M HCl. The prepared solutions were stirred for 24 h. On the day of deposition, 2 wt% AG solution at pH 4 was prepared using 0.1 M HCl. (0.25 % CH - 1 % AG) at pH 4 was prepared by mixing equal amounts of 0.5 wt% chitosan and 2 wt% AG, while (0.25 % P - 1 % AG) at pH 4 was done by mixing an equal amounts of 0.5 wt% pectin and 2 wt % AG dye.

2.2.2. LbL deposition

TheLbL deposition was performed by deep coating a strip of cotton fabric with dimensions 18 cm x 8 cm (1.94 g) in two oppositely charged aqueous solutions, with rinsing in between (Fig. 1). One bilayer (BL) is formed when the fabric is hand-dipped in a positively charged solution for 5 min, then rinsed in DI water, followed by another 5 min immersion in a negatively charged solution and another rinsing. The duration of the immersion for the following layers (after the first BL) is 1 min. The polyelectrolyte solutions and the DI water were changed according to the number of total BL. For 2 and 4 BL, the solutions were not renewed. For 6 and 8 BL, solutions were changed after the third and fourth BL, respectively). After the LbL deposition was done, the samples were air-dried at room temperature ($21 \, °C \pm 1 \, °C$).

2.2.3. Conventional dyeing of the cotton fabric with AG

To compare 8BL LbL-dyed with the conventional (traditional) dyed cotton, the cotton sample was dyed in the Linitest apparatus for 30 min at 21 °C with 2 % AG dye in a bath with a 1:30 liquor ratio. The time of conventional dyeing was the same as the time it takes to deposit 8 BL of $(CH-AG)_4/(P-AG)_4$.

2.2.4. Preparation of buffer solutions

All buffer solutions had a molarity of 0.1 M. The pH 3 buffer was prepared with glycine and citric acid. The pH 4 and 5 buffers were made with sodium acetate and acetic acid. Monopotassium phosphate and sodium hydroxide were used for the pH 6 and 7 buffers. The pH 8 and 9 buffers were obtained by mixing borax and boric acid, while the pH 10 buffer was made using borax and sodium hydroxide.

2.2.5. Treatment of 8BL $(CH-AG)_4/(P-AG)_4$ coated cotton fabric in different buffers

Coated cotton fabric strips with dimensions 2 cm x 8 cm (0.23 g) were dipped into Petri dishes filled with different buffers for 20 s and left to air-dry. All prepared buffers (pH 3, 4, 5, 6, 7, 8, 9, and 10) had a molarity of 0.1 M, adjusted with addition of 0.1 M HCl and 0.1 M NaOH aqueous solutions. The color of the coated samples started to change immediately and it was complete after 5 s. To be sure that color is unchangeable, the samples were kept in buffers for 20 s.

2.3. Characterization

2.3.1. pH measuring

The pH of the buffer solutions was measured with an HI 9321 Microprocessor-based Bench pH meter from HANNA Instruments, Leighton, UK.

2.3.2. VIS-spectroscopy

The VIS-spectrophotometric scanning of the solutions with AG-dye in different buffers was done with Drawell UV/VIS Spectrophotometer DU-8200 (Shanghai, China), in a wavelength range from 400 nm to 750 nm.

2.3.3. Scanning electron microscopy (SEM)

SEM was performed using a TESCAN VEGA 3 LMU electron microscope (Brno, Czech Republic) with a beam voltage of 5 kV. To prevent surface charging, a gold coating of the sample before imaging was applied.

2.3.4. Fourier transform infrared-attenuated total reflectance (FTIR-ATR) spectroscopy

FITR-ATR was performed on uncoated and coated fabric samples using a Nicolet 370 FTIR Spectrometer (Thermo Scientific, Waltham, MA, USA) at 4 cm^{-1} resolution, over the range of 500–4000 cm^{-1}.

2.3.5. CIELab color coordinates of the dyed fabrics

CIELab coordinates (L*, a*, b*, C*, h) and K/S were used as a parameters for characterization the color of the dyed cotton samples. These parameters were determined by spectrophotometer (X-Rite Color i7 Spectrophotometer, Kentwood, MI, USA) under illuminant D_{65} using the 10° standard observer. The L* value represents the lightness of the dyed simple. Lower L* values indicate more colored samples. a* is chromatic green (-a*) - red (+a*) axis, while b* is chromatic blue (-b*) – yellow (+b*) axis. C* is saturation and h is hue of the colored surface.

The K/S was calculated from the reflectance values using the Kubelka−Munk equation

$$\frac{K}{S} = \frac{(1-R)^2}{2R}$$

where R is the reflectance, K is the absorption coefficient, and S is the light scattering coefficient. The presented results are the mean values of five measurements.

The color difference (ΔE*) between the fabrics after and before subjecting them to buffers with different pH was determined using the equation:

$$\Delta E^* = \sqrt{(\Delta a*)^2 + (\Delta b*)^2 + (\Delta L*)^2} \tag{1}$$

where: ΔL* - the lightness difference; Δa* - red/green difference; Δb* - yellow/blue difference.

2.3.6. Antimicrobial activity

The antimicrobial activity of the samples was tested against Gram-negative bacteria *E. coli* (ATCC 25922), Gram-positive bacteria *S. aureus* (ATCC 25923) and yeast *C. albicans* (ATCC 24433) according to ASTM E 2149-01. Bacteria and yeast inocula were prepared in tryptone soy broth (Torlak, Serbia), and applied as the growth medium for microorganisms. A physiological saline solution (pH 7.2) was used as a testing medium. Microorganisms were cultivated for 18 h (late exponential stage of growth) in 3 mL of tryptone soy broth at 37 °C. 50 mL of sterile physiological saline solution was inoculated with 0.5 mL of microbial inocula. After sterilization (UV light for 30 min), the samples were put in the flasks filled with the inoculated sterile physiological saline solution and shaken at 37 °C for 2 h. The aliquots from the flasks were diluted with physiological saline solution and placed (1 mL) onto a tryptone soy agar. The initial number of bacteria or yeast colonies was obtained by taking 1 mL aliquots from the inoculum (expressed in CFU/mL), which were diluted with physiological saline solution, and placed onto a tryptone soya agar. The number of microbial colonies was counted after a 24 h incubation at 37 °C. The percentage of microbial reduction (R,%) was calculated in accordance with the following equation:

$$R = \frac{C_0 - C}{C_0} \times 100 \tag{2}$$

where: C_0 (CFU/mL - colony forming units in 1 mL aliquots) is the number of microorganisms that were in the contact with the control sample (uncoated cotton fabric) and C (CFU/mL) is the number of microorganisms that were in contact with the coated samples (8BL CH_4/P_4 and 8BL $(CH-AG)_4/(P-AG)_4$).
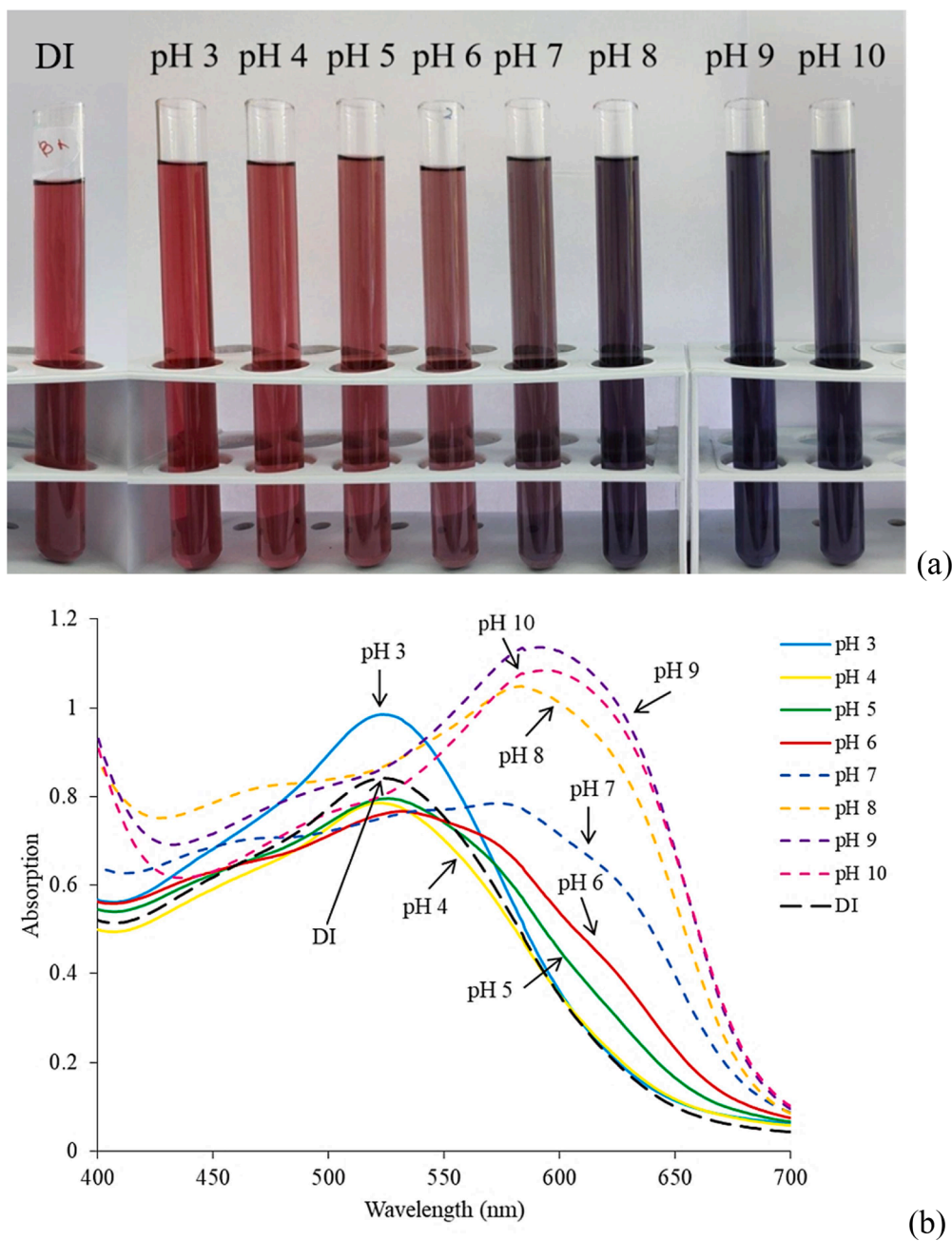
Fig. 2. Image of AG-dye dissolved in DI water and in buffers with pH 3 to pH 10 (a) and their VIS-absorption spectra (b).

2.3.7. Cytotoxicity

The cytotoxicity of the cotton fabric, LbL coated (with and without AG dye) was evaluated as described elsewhere (Ivanoska-Dacikj et al., 2022; Marković et al., 2023) with slight modifications and in accordance with ISO 10993-5-2009. The 2 cm×2 cm samples from the fabrics were placed in 100 mL sterile test tubes and incubated with various volumes (22, 45, and 67 mL) of complete cell culture medium (DMEM supplemented with 10 % FBS, pen/strep/ampB) on 37 °C with continuous agitation at 50 rpm in a horizontal shaking water bath (Haake, Denmark) for 24 h. Afterwards, the liquid extracts were filtered through 0.2 μm regenerated cellulose (RC) membrane filters under aseptic conditions and further used for cytotoxicity evaluation. The human fibroblast cell line (MRC-5) was grown in complete DMEM at 37 °C, 5 % CO_2, and 90 % relative humidity in a CO_2 incubator (MRC, Israel). After reaching confluence, the cells were detached using trypsin/EDTA solution, transferred to complete DMEM, centrifuged, and dispersed again in complete DMEM. The cells were seeded in 96 well plates at a density of 5000 cells/well, left for 18 h to attach, and afterwards, the medium was aspirated and replaced with the appropriate liquid extract (0.2 mL/well) and incubated for 48 h. The cell culture medium was used as blank, while high-density polyethylene (65 mg/22 mL) was used as negative and Triton X-100 (0.2 %) as a positive control to demonstrate the suitability of the assay in terms of appropriate response, possible confounding effects and background effect. The cell viability was determined following the standard MTT assay protocol, where 0.02 mL of the MTT solution (4 mg/mL) was added to each well and allowed to incubate for a further 4 h at 37 °C, 5 % CO_2, and 90 % relative humidity in a CO_2 incubator. Afterwards, the medium was removed and 0.2 mL of DMSO was added to each well to solubilize the formazan crystals. The absorbance intensity of each well was measured at a wavelength of 560 nm using a Victor X4 multi-plate reader (Perkin Elmer MA, USA). The cell morphology was observed using an inverted microscope CX 43
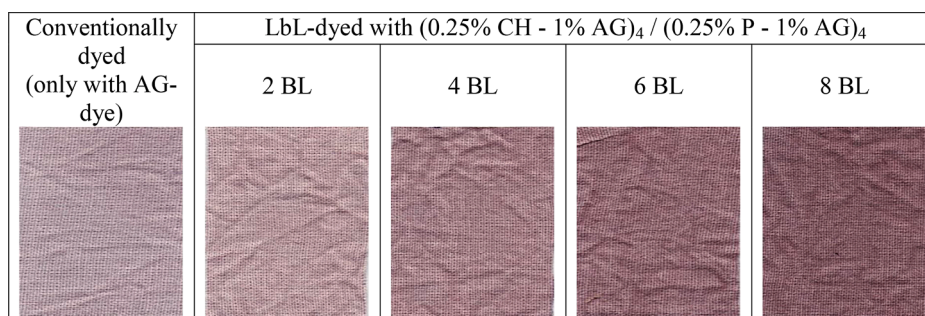
Conventionally dyed (only with AG-dye)	LbL-dyed with (0.25% CH - 1% AG)₄ / (0.25% P - 1% AG)₄			
	2 BL	4 BL	6 BL	8 BL

Fig. 3. Images of conventionally dyed (with AG-dye) and LbL-dyed samples with 2, 4, 6 and 8 BL of (CH -AG)₄ / (P - AG)₄. (The magnification factor of these images is 20X).

(Olympus, Japan) equipped with a CCD camera. In addition, to explore possible chemical alterations (polymer dissociation, interactions with sera proteins from the cell culture medium) after the extraction procedure, each fabric sample was rinsed with DI water, air dried, and scanned with ATR-FTIR (described previously), and Raman spectroscopy on ATR 3000 DH (Optosky, China) using the following parameters: laser power 400 mW, integration time 60 s, and excitation time 60 s.

3. Results and discussion

3.1. Color change of AG-dye solution vs. pH (in aqueous buffers)

Anthocyanins are glycosylated polyhydroxy and polymethoxy derivatives of 2-phenylbenzopyrylium (flavylium) salt that contain conjugated double bonds, resulting in an absorption of visible light at a wavelength of around 500 nm (Favaro et al., 2018). They differ in the number of hydroxyl groups, the nature, number, and position of the sugars attached to the molecule, and the nature and number of aliphatic or aromatic acids attached to sugars in the molecule. These factors influence the color of the pigment and are responsible for the changes in color at different pH (de Lima et al., 2007). The positive charge on the internal ring of the anthocyanin molecule, which is pH-dependent, is responsible for its pigmentation and is neutralized at a higher pH (Favaro et al., 2018). To test the color change of the anthocyanin grape (AG) dye against pH, 2 % of this dye was dissolved in DI water and pH 3, 4, 5, 6, 7, 8, 9, and 10 buffer solutions (Fig. 2(a)). As the pH value of the buffers increases, an obvious, with the naked eye, color change from pink to violet-blue is noticed between pH 6 and 7. This color change was also instrumentally assessed. The VIS spectra of AG-dye show a noticeable shift in the wavelength of maximum absorption from pH 6 to 7 (Fig. 2(b)). VIS spectra of AG-dye dissolved in DI water and in pH 3, 4, and 5 buffer solutions have maximum absorption at around 520 nm. The maximum absorption of the VIS-spectra of AG-dye dissolved in pH 6 buffer solution is moved to 530 nm, while the VIS-spectra of AG-dye

dissolved in pH 7 buffer solution has a new shape with an absorption maximum of around 570 nm. As pH increases, the maximum absorption of VIS-spectra in pH 8, 9, and 10 buffer solutions have moved to around 600–610 nm. Since the transition of the color of AG-dye (pH 6 to 7) fits quite well with the pH of the heal-infected wound, this natural dye can be used in pH-indicating wound dressing.

3.2. Conventionally dyed (with AG-dye) and LbL-dyed cotton with (CH-AG)₄/(P-AG)₄

As already mentioned, the normally healing wound has a pH of around 4 to 6, while an infected one has a pH above 7. Many pH-indicating dyes change the color at pH 6, 7, which is the pH transition of the healing to an infected wound. Only some types of those dyes, which possess good exhaustion into textile fibers, antimicrobial properties and no cytotoxicity, can be used for wound dressing. Since AG-dye is a natural dye with limited groups capable of creating bonds with the fiber, the substantivity of AG-dye to the cellulosic cotton fiber is very low, and the conventional dyeing process is not easy to conduct. The LbL assembly, with its step-by-step application of the AG dye on the surface of the cotton fabric, is a good approach to overcome this drawback. To compare the traditional and LbL dyeing, the cotton sample was dyed conventionally in the Linitest apparatus for 30 min at 21 °C with 2 % AG dye in a bath with a 1:30 liquor ratio. The time of conventional dyeing was similar to the time it takes to deposit 8 BL. The optimal number of applied BL was chosen when the cotton fabric was coated with 2, 4, 6, and 8 BL of CH₄/P₄ and (CH-AG)₄/(P-AG)₄. The images of conventionally and LbL-dyed cotton with AG-dye are presented in Fig. 3. The conventionally dyed cotton has a similar color as 2 BL dyed cotton with (CH-AG)₄/(P-AG)₄ (Fig. 3). This fabric has L* 70.72, a* 11.9, b* -2.57, C* 12.15, h 347.8 and K/S 0.71. As the number of the BL increase, the color yield of the LbL-coated cotton fabrics dramatically increases (Fig. 3). The weight gain and CIELab color coordinates measured by reflection spectrophotometer for the CH₄/P₄ and (CH-AG)₄/(P-AG)₄

Table 1

CIELab color coordinate of CH₄/P₄ and (CH-AG)₄/(P-AG)₄ LbL-coated cotton fabrics.

BL	0.25 % CH₄ / 0.25 % P₄					(0.25 % CH - 1 % AG)₄ / (0.25 % P - 1 % AG)₄									
	WG (%)	L^*	a^*	b^*	ΔE (BL$_X$/ BL$_2$)	WG (%)	AG-dye (%)	L^*	a^*	b^*	C^*	h	K/S^*	ΔE (with and without AG)	ΔE (BLx/ BL$_2$)
2	0.67 ± 0.03	94.4 ± 0.32	−0.09 ± 0.01	3.69 ± 0.13		1.45 ± 0.09	0.78 ± 0.03	70.6 ± 0.45	12.13 ± 0.29	−1.68 ± 0.08	12.25 ± 0.29	352.1 ± 2.26	0.74 ± 0.03	27.25 ± 0.56	
4	1.42 ± 0.07	94.2 ± 0.43	−0.11 ± 0.02	4.02 ± 0.15	0.36 ± 0.02	2.11 ± 0.11	0.69 ± 0.02	65.0 ± 0.52	12.67 ± 0.26	−1.32 ± 0.06	12.73 ± 0.26	354.1 ± 1.59	0.94 ± 0.06	32.32 ± 0.64	5.62 ± 0.16
6	2.13 ± 0.10	94.3 ± 0.22	−0.09 ± 0.01	3.95 ± 0.11	0.28 ± 0.01	3.52 ± 0.14	1.39 ± 0.04	59.9 ± 0.36	13.46 ± 0.33	−0.99 ± 0.03	13.49 ± 0.38	355.8 ± 1.88	1.39 ± 0.08	37.23 ± 0.75	10.78 ± 0.24
8	2.92 ± 0.13	94.0 ± 0.36	−0.21 ± 0.02	4.45 ± 0.16	0.86 ± 0.04	4.89 ± 0.21	1.97 ± 0.06	56.1 ± 0.39	13.65 ± 0.37	−1.25 ± 0.05	13.71 ± 0.39	354.8 ± 2.03	1.74 ± 0.10	40.77 ± 0.66	14.62 ± 0.33

* K/S is Kubelka-Munk value used as an indicator of color yield.
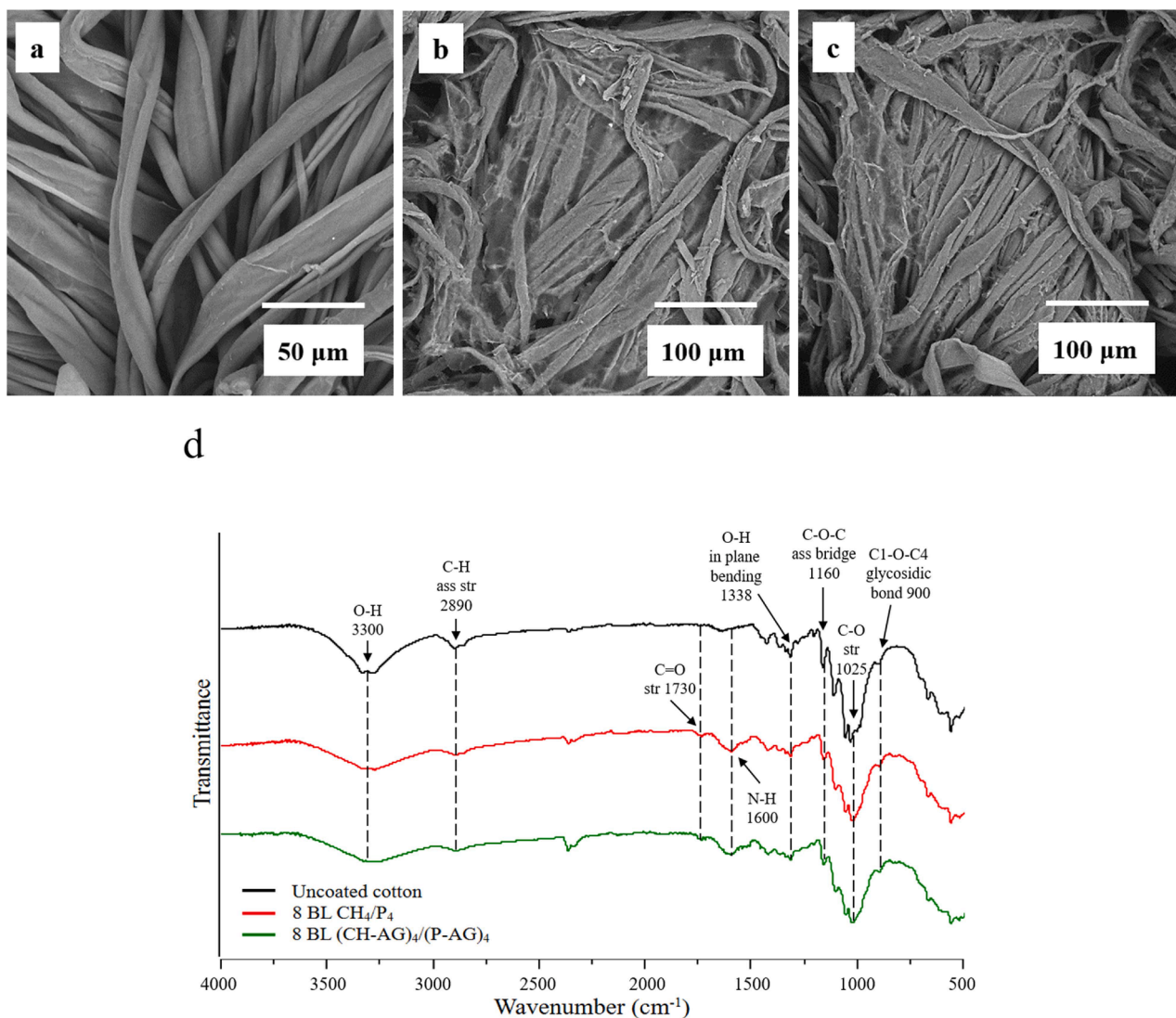
Fig. 4. SEM images of uncoated (a) and cotton fabric coated with 8 BL of CH$_4$/P$_4$ (b); and 8 BL of (CH-AG)$_4$/(P-AG)$_4$ (c) and their FTIR spectra (d). The magnification of the SEM image under (a) is 1000X, while the magnification of the images under (b) and (c) is 500X.

coated samples are shown in Table 1. The weight gain of CH$_4$/P$_4$ and (CH-AG)$_4$/(P-AG)$_4$ samples increased gradually with the number of BL deposited, with the highest weight gain being 2.92 wt% for 8 BL CH$_4$/P$_4$ and 4.89 wt% weight gain of 8BL (CH-AG)$_4$/(P-AG)$_4$. Hypothetically, the difference between weight gain of (CH-AG)$_4$/(P-AG)$_4$ and CH$_4$/P$_4$ (at the same number of deposited BL) is the amount of AG-dye deposited on the surface of cotton fiber via LbL assembly. For 8 BL-coated cotton fabric the amount of deposited AG-dye is 1.97 wt%. For comparison, the weight gain of traditionally dyed cotton with 2 % AG-dye is 0.64 wt%. The CH$_4$/P$_4$ coated samples are white with L (light) values of more than 94 (Table 1). As the number of BL increases, the CIELab coordinates of these samples do not change substantially. ΔE values obtained between 4, 6, and 8 BL of CH$_4$/P$_4$ coated fabrics relative to 2 BL are less than 2, indicating not with naked eye visible changes. The ΔE, which quantifies the difference between (CH-AG)$_4$/(P-AG)$_4$ and CH$_4$/P$_4$ coated samples, started from 27.25 for 2 BL and went up to 40.77 for 8 BL coated cotton fabrics. Opposite to CH$_4$/P$_4$, ΔE values obtained between 4, 6, and 8 BL relative to 2 BL (CH-AG)$_4$/(P-AG)$_4$ coated cotton fabrics are higher than two and have values of 5.62, 10.78 and 14.62, for 4, 6 and 8 BL, respectively.

3.3. Characterization of the coatings by SEM and FTIR-ATR spectroscopy

Fig. 4 (a–c) shows the SEM micrographs of uncoated (Fig. 4(a)) and cotton samples coated with 8 BL of CH$_4$/P$_4$ (Fig. 4(b)) and (CH-AG)$_4$/(P-AG)$_4$ (Fig. 4(c)). Although CH$_4$/P$_4$ and (CH-AG)$_4$/(P-AG)$_4$ samples seems to have similar coatings, the coating of 8 BL (CH-AG)$_4$/(P-AG)$_4$ coated cotton fabric looks more conformally, which means that this coating covers each fiber more individually, rather than creating inter-fiber bridges. FTIR-ATR spectra of uncoated and LbL-coated cotton are shown in Fig. 4(d). The peaks that appear in the spectra for the uncoated cotton are all characteristic peaks for cotton reported in the literature (Jordanov & Mangovska, 2011; Petkovska et al., 2022). A peak at 1730 cm^{-1} is attributed to the stretching vibration of the C=O group of carboxylate functional groups (COO$^-$) in the pectin structure (Duwee et al., 2022). The peak that appears at 1600 cm^{-1} is attributed to the bending vibration of the N-H group in a primary amine, which is an indication of the presence of chitosan (Petkovska et al., 2023). The dyed sample presented the same peaks as the sample coated with only chitosan and pectin, without a characteristic peak for anthocyanin.

Table 2
Images (magnification 10X) and CIELab color coordinates of 8 BL (CH-AG)$_4$/(P-AG)$_4$ coated cotton fabric subjected to different pH buffers.

	Control (DI water)	Buffer						
		pH 4	pH 5	pH 6	pH 7	pH 8	pH 9	pH 10
Image								
$L*$	57.84 ± 0.76	58.82 ± 0.69	59.91 ± 0.88	59.72 ± 0.58	58.01 ± 0.79	60.53 ± 0.47	59.83 ± 0.95	62.71 ± 0.83
$a*$	12.03 ± 0.39	9.91 ± 0.22	8.48 ± 0.15	8.10 ± 0.19	5.50 ± 0.11	4.04 ± 0.08	1.98 ± 0.04	−0.69 ± 0.02
$b*$	0.55 ± 0.04	0.89 ± 0.04	0.59 ± 0.01	0.41 ± 0.01	0.27 ± 0.01	0.08 ± 0.01	0.70 ± 0.03	0.25 ± 0.01
$C*$	12.05 ± 0.28	9.95 ± 0.31	8.50 ± 0.24	6.41 ± 0.19	5.52 ± 0.17	4.05 ± 0.15	2.10 ± 0.09	0.80 ± 0.03
h	2.61 ± 0.11	5.13 ± 0.19	3.96 ± 0.15	2.75 ± 0.12	4.77 ± 0.17	1.18 ± 0.04	19.40 ± 0.49	149.7 ± 2.78
K/S	1.40 ± 0.06	1.37 ± 0.06	1.31 ± 0.05	1.42 ± 0.03	1.55 ± 0.04	1.33 ± 0.02	1.44 ± 0.03	1.44 ± 0.03
ΔE (pHx/pH4)	–	–	1.82 ± 0.09	2.08 ± 0.10	4.53 ± 0.20	6.17 ± 0.29	7.99 ± 0.30	11.31 ± 0.41
ΔE (pHx/pH6)	–	–	–	–	3.12 ± 0.13	4.15 ± 0.16	6.13 ± 0.19	9.28 ± 0.26

Table 3
Antimicrobial activity of uncoated and LbL-coated cotton fabrics.

Sample	Microorganism					
	E. coli (ATCC 25922)		*S. aureus* (ATCC 25923)		*C. albicans* (ATCC 24433)	
	CFU/mL	R (%)	CFU/mL	R (%)	CFU/mL	R (%)
Inoculum	3.0×10^6		9.2×10^5		1.3×10^6	
Control	6.5×10^6		2.0×10^5		2.2×10^5	
8BL CH$_4$/P$_4$	4.9×10^5	92.5	2.4×10^3	98.8	8.6×10^3	96.1
8BL (CH-AG)$_4$/(P-AG)$_4$	6.35×10^5	90.2	800	99.6	<10	99.9

3.4. pH indicating ability of (CH-AG)$_4$/(P-AG)$_4$ coated cotton fabric

Since the 8 BL (CH-AG)$_4$/(P-AG)$_4$ coated sample has the most intensive color, this fabric was soaked in different pH buffers, and the color change, evident to the naked eye, was photographed and quantified by reflection spectrophotometer (Table 2). The color of pH-indicating cotton fabric is pink when it is subjected to pH 3–6 buffers. Violet-blue color started to develop when the sample was soaked in a pH 7 buffer. This color becomes bluer as the pH of buffers increases from 8 to 10 (Table 2). CIELab coordinates of 8 BL (CH-AG)$_4$/(P-AG)$_4$ coated cotton fabric subjected to different pH buffers are presented in Table 2. The $L*$ values after buffering are slightly changed. The $a*$ value, which is an indicator of the red-green component of the color, decreases with a higher pH value, meaning that the samples were gradually losing their red component. The $b*$ value, or the indicator of yellow-blue components, also decreases as the pH of the buffer increases, confirming the transition of the pigment to a bluer shade. The saturation of the color ($C*$) decreases at a higher pH while the hue (h) increases drastically above pH 8. The similar K/S values to all buffered samples indicate no significant change in the color yield. Color difference, ΔE, calculated relative to LbL-dyed cotton fabric buffered at pH 4, increases as the pH of the buffers rises. Up to pH 6, the color difference is about 2, indicating no visible changes in the color. When the LbL-dyed cotton is buffered from pH 7 to 10, the color differences relative to pH 4 are visible and higher than 2. To assess the potential of 8 BL (CH-AG)$_4$/(P-AG)$_4$ dyed cotton to be used as pH indicating wound dressing, ΔE between this fabric subjected to pH 6 and 7 buffers is presented in the last row of Table 2. The color difference $\Delta E_{pH7/pH6}$ is higher than 3, suggesting a visible transitions of the color from pink to violet-blue in this pH region.

3.5. Antimicrobial properties

The results from the antimicrobial activity of coated and uncoated cotton against Gram-negative bacteria E. coli, Gram-positive bacteria S. aureus, andC. albicansyeast, are summarized in Table 3. The uncoated cotton does not show any antimicrobial activity. The LbL-coated samples (without and with AG-dye) exhibit bacteriostatic effects againstE. coli, antibacterial activity againstS. aureus, and antifungal activity againstC. albicans. The presence of chitosan and pectin in 8 BL CH$_4$/P$_4$ coated fabric is responsible for its antimicrobial activity. The electrostatic interaction between the positive charges from the amino groups of chitosan and negatively charged components on the microbial membrane causes the antimicrobial action of chitosan (Yan et al., 2021). Pectin has also been reported as an efficient antimicrobial agent against yeasts, Gram-negative bacteria, and non-filamentous fungi. It has been attributed to the binding action of the carboxylic acid groups in the main backbone of the biopolymer (Ciriminna et al., 2020). The addition of anthocyanin in the chitosan/pectin recipe improves already satisfactory antimicrobial activity of this polyelectrolyte complex. The phenolic compounds and organic acids from anthocyanins are responsible for
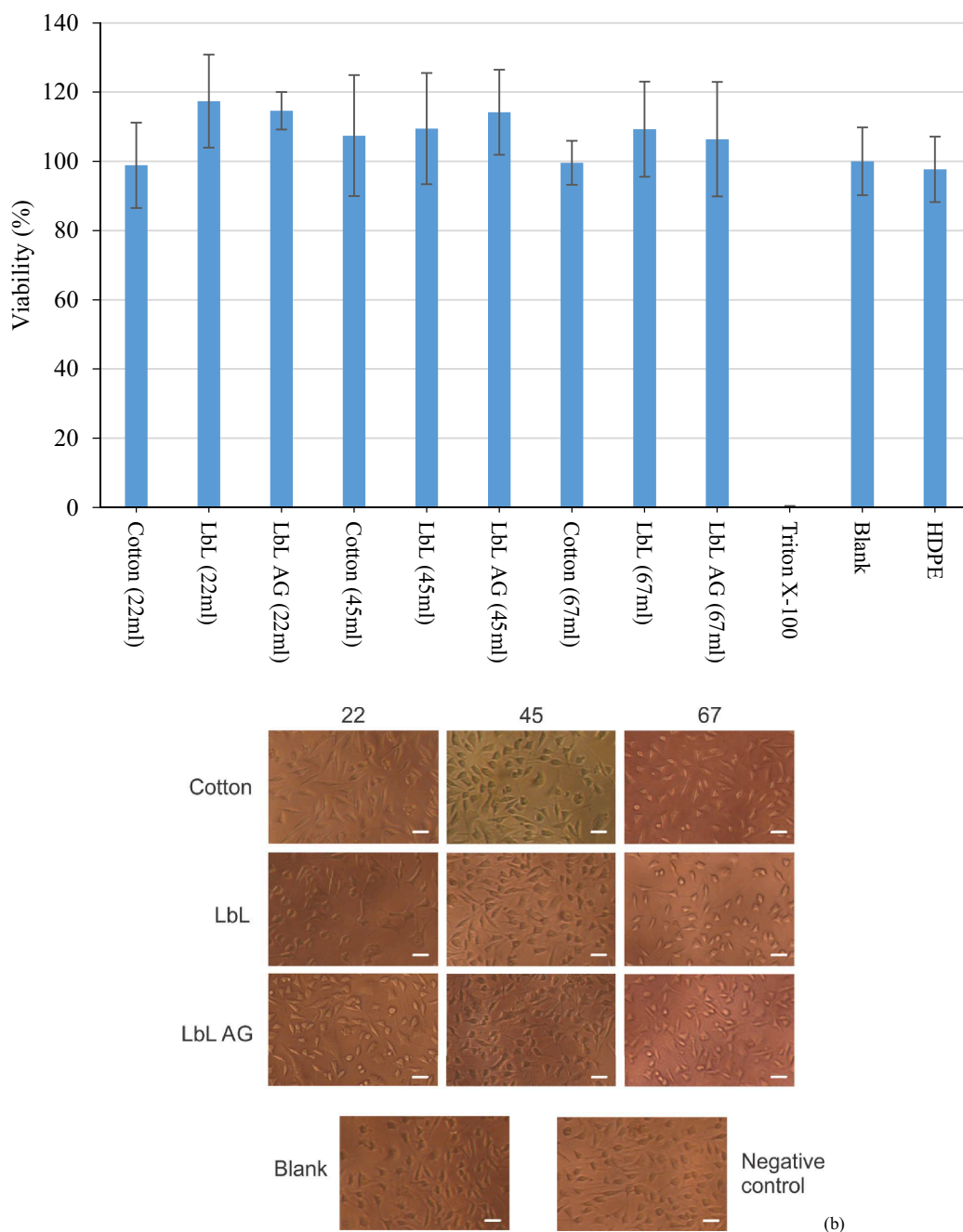
Fig. 5. (a) Viability of the MRC-5 cells treated with different volumes of extraction media (22, 45, and 67 ml) from cotton fabric (Cotton), 8 BL CH$_4$/P$_4$ (LbL) and 8 BL (CH-AG)$_4$/(P-AG)$_4$ (LbL AG). Triton X-100 and HDPE were used as positive and negative control, respectively. ($n = 8$); (b) Morphology of the MRC-5 cells treated with different volumes of extraction media (22, 45 and 67 ml) after 48 h of incubation. Cell morphology images in the blank experiments (media only) and the negative control (HDPE) are also presented. (Magnification 40X and scale bar = 20 μm).

their antimicrobial activity (Favaro et al., 2018). Obtained results indicate that the presence of chitosan, pectin, and anthocyanin on the surface of the cotton fabric suffices to impart bacteriostatic to slightly antibacterial activity against *E. coli*, good antibacterial activity against *S. aureus* and excellent antifungal properties (99.9 %) to the potential wound dressing after only 2 h contact.

3.6. Cytotoxicity

The results from the cytotoxicity evaluation are presented in Fig. 5 (a). The liquid extracts from all evaluated samples demonstrate no cytotoxic effect on the cell line MRC-5, as there is no statistically

significant difference between the blank and negative control ($p < 0.05$). The samples with adsorbed chitosan demonstrate increased cell proliferation, probably due to the stimulative effects of the chitosan on the cells (Debnath et al., 2015; Gjoseva et al., 2018), which is negligible. The morphological evaluation of the cells treated with extracts from the fabrics do not reveal any signs of cell death, apoptosis or reduction of normal proliferation relative to the blanks and negative control (Fig. 6 (b)) thus confirming the results from the MTT assay.

The FTIR-ATR (Fig. 6) and Raman spectra (Fig. 7) revealed no notable chemical alterations of the samples after incubation with different volumes of complete DMEM (i.e. elution of the adsorbed chitosan and pectin). In addition, no characteristic bands of the serum
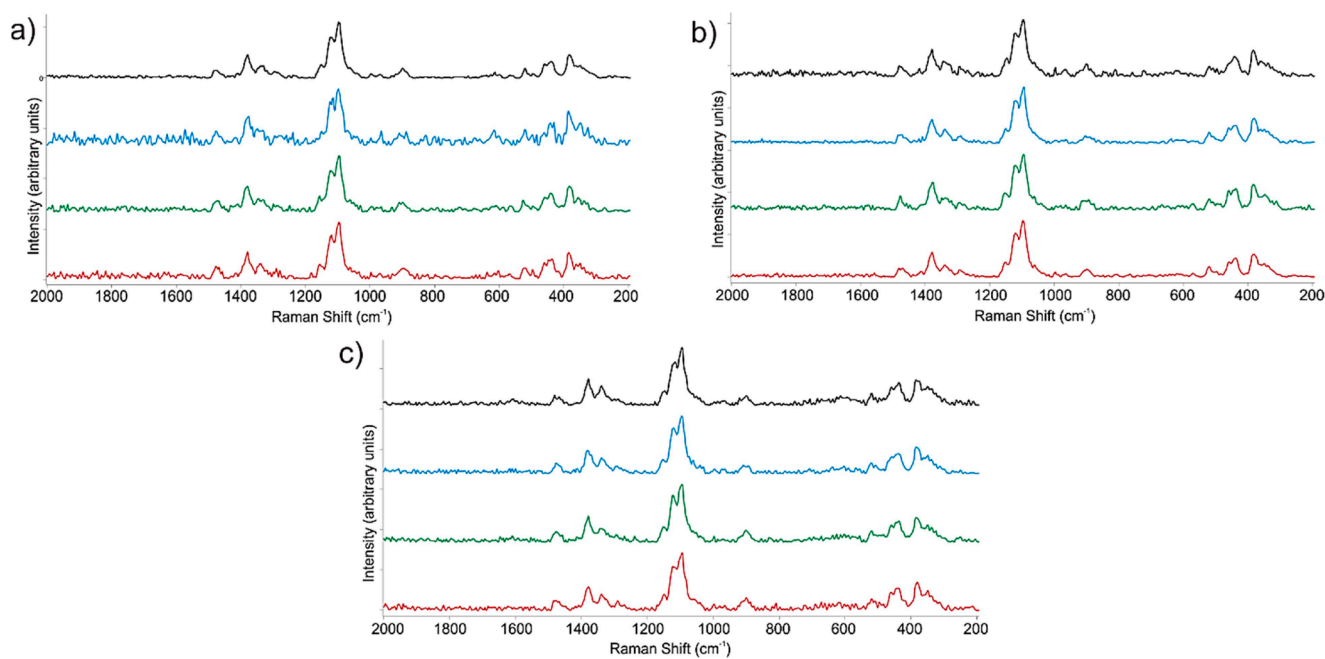
Fig. 6. FTIR-ATR spectra of fabrics prior to (black), and after incubation with cell culture media with 22 ml (blue), 45 ml (green) and 67 ml (red); a) cotton, b) 8 BL CH_4/P_4 and c) 8 BL $(CH-AG)_4/(P-AG)_4$.
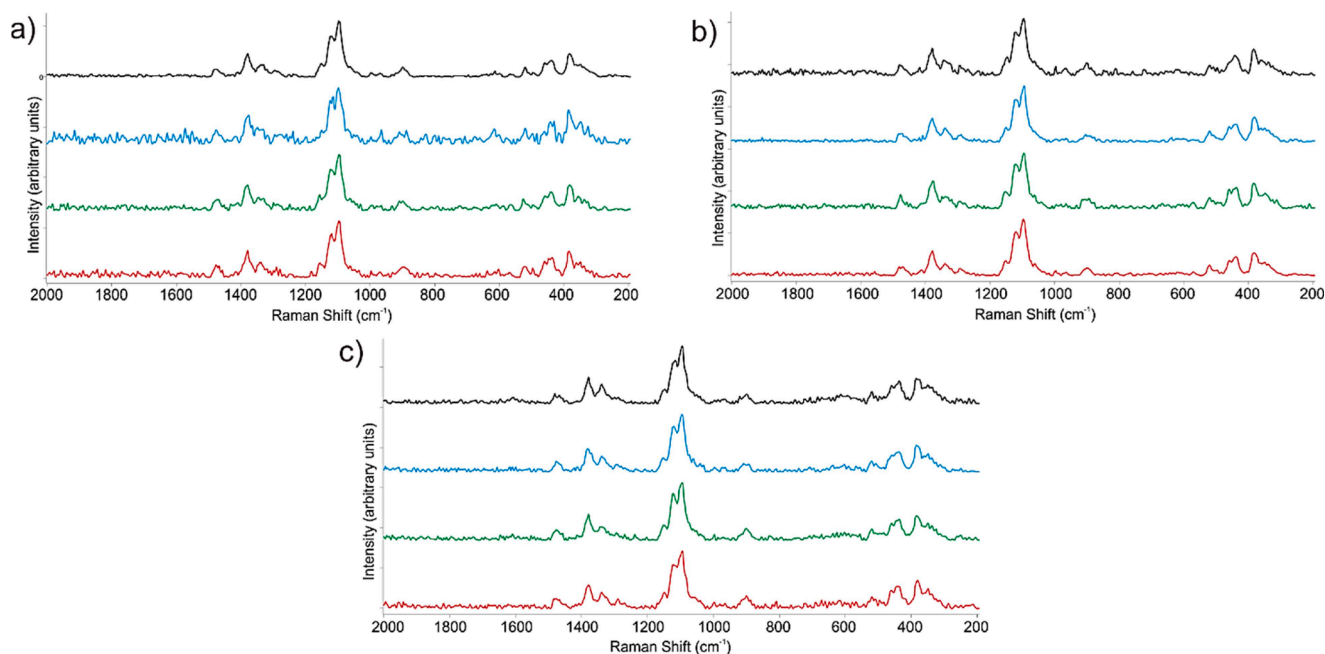
Fig. 7. Raman spectra of fabrics prior to (black), and after incubation with cell culture media with 22 ml (blue), 45 ml (green) and 67 ml (red); a) cotton, b) 8 BL CH_4/P_4 and c) 8 BL $(CH-AG)_4/(P-AG)_4$.

proteins appeared, thus indicating that there was no significant interaction with the cell culture medium components. Taking into account the above results, one could presume that the prepared fabric samples are stable in the biological environment and do not elute components that could be cytotoxic.

4. Conclusions

pH-indicating wound dressing was fabricated by applying chitosan, pectin, and anthocyanin dye on the surface of the cotton fabric using a layer-by-layer assembly. 8 BL of (0.25 % CH-1 % AG)₄/(0.25 % P-1 %

AG)₄ nanocoating imparted 1.97 wt% AG-dye with an intensive pink color of the cotton fabric. VIS-spectra of anthocyanin dye in aqueous buffers has maximum adsorption of 520 nm at pH 3 to 5, which moves to 530 nm at pH 6, 570 nm at pH 7, and 600–610 nm at pH 8 to 10. The change of the color of buffered LbL-dyed cotton fabric behaves the same as the color change of the anthocyanin in buffers. The pink color at pH 3 to 6 immediately changes to violet-blue when pH increases from 6 to 7 and becomes bluer in the pH range from 7 to 10. The color difference is the most intense between pH 6 and 7, with CIE color difference larger than 3. The pH of the color transition of 8 BL $(CH-AG)_4/(P-AG)_4$ LbL-coated cotton is the same as the pH transition of normal healing to an

infected wound. Therefore, this nanocoating can be efficiently used for the fabrication of pH-indicating wound dressing. This pH-indicating wound dressing possesses slight antimicrobial activity against Gram-negativebacteria E. coli, good antimicrobial activity against Gram-positive bacteriaS. aureus, and excellent antifungal activity against C. albicans. Since this cotton fabric is coated with bio-sourced chemicals known for their anti-infecting properties, this pH-indicating wound dressing shows no cytotoxicity on MRC-5 cells. In the future, this examination should be a solid base for creating bio-sourced pH-indicating wound dressing with improved healing behavior using medicaments within the porous layer-by-layer network of polyelectrolytes.

Funding sources

CRediT authorship contribution statement

Jovana Petkovska: Investigation, Data curation, Writing – original draft. **Nikola Geskovski:** Data curation. **Darka Marković:** Data curation. **Vesna Dimova:** Data curation. **Dejan Mirakovski:** Data curation. **Maja Radetić:** Data curation, Writing – review & editing. **Igor Jordanov:** Conceptualization, Supervision, Writing – review & editing.

Declaration of competing interest

The authors declare that they have no known competing financial interests or personal relationships that could have appeared to influence the work reported in this paper.

Data availability

Data will be made available on request.

References

Arafa, A. A., Nada, A. A., Ibrahim, A. Y., Sajkiewicz, P., Zahran, M. K., & Hakeim, O. A. (2021). Preparation and characterization of smart therapeutic pH-sensitive wound dressing from red cabbage extract and chitosan hydrogel. *International Journal of Biological Macromolecules, 182*, 1820–1831. https://doi.org/10.1016/j.ijbiomac.2021.05.167

Bennison, L. R., Miller, C. N., Summers, R. J., Minnis, A. M. B., Sussman, G., & McGuiness, W. (2020). The pH of wounds during healing and infection: A descriptive literature review. *Wound Practice & Research: Journal of the Australian Wound Management Association, 25*(2), 63–69. https://doi.org/10.3316/informit.927380056251808

Bowler, P. G., Duerden, B. I., & Armstrong, D. G. (2001). Wound microbiology and associated approaches to wound management. *Clinical Microbiology Reviews, 14*(2), 244–269. https://doi.org/10.1128/cmr.14.2.244-269.2001

Ciriminna, R., Fidalgo, A., Meneguzzo, F., Presentato, A., Scurria, A., Nuzzo, D., et al. (2020). Pectin: A long-neglected broad-spectrum antibacterial. *ChemMedChem, 15*(23), 2228–2235. https://doi.org/10.1002/cmdc.202000518

Cui, L., Hu, J., Wang, W., Yan, C., Guo, Y., & Tu, C. (2020). Smart pH response flexible sensor based on calcium alginate fibers incorporated with natural dye for wound healing monitoring. *Cellulose, 27*(11), 6367–6381. https://doi.org/10.1007/s10570-020-03219-1

de Lima, A. A., Sussuchi, E. M., & De Giovani, W. F. (2007). Electrochemical and antioxidant properties of anthocyanins and anthocyanidins. *Croatica Chemica Acta, 80*(1), 29–34.

Debnath, T., Ghosh, S., Potlapuvu, U. S., Kona, L., Kamaraju, S. R., Sarkar, S., et al. (2015). Proliferation and differentiation potential of human adipose-derived stem cells grown on chitosan hydrogel. *PloS One, 10*(3), Article e0120803. https://doi.org/10.1371/journal.pone.0120803

Derakhshandeh, H., Kashaf, S. S., Aghabaglou, F., Ghanavati, I. O., & Tamayol, A. (2018). Smart bandages: The future of wound care. *Trends in Biotechnology, 36*(12), 1259–1274. https://doi.org/10.1016/j.tibtech.2018.07.007

Duwee, Y. S., Kiew, P. L., & Yeoh, W. M. (2022). Multi-objective optimization of pectin extraction from orange peel via response surface methodology: Yield and degree of esterification. *Journal of Food Measurement and Characterization, 16*(2), 1710–1724. https://doi.org/10.1007/s11694-022-01305-5

Favaro, L., Balcão, V., Rocha, L., Silva, E., Oliveira, J., Jr, Vila, M., et al. (2018). Physicochemical characterization of a crude anthocyanin extract from the fruits of jussara (Euterpe edulis Martius): Potential for food and pharmaceutical applications. *Journal of the Brazilian Chemical Society.* https://doi.org/10.21577/0103-5053.20180082

Gamerith, C., Luschnig, D., Ortner, A., Pietrzik, N., Guse, J. H., Burnet, M., et al. (2019). pH-responsive materials for optical monitoring of wound status. *Sensors and Actuators B: Chemical, 301*, Article 126966. https://doi.org/10.1016/j.snb.2019.126966

Gjoseva, S., Geskovski, N., Sazdovska, S. D., Popeski-Dimovski, R., Petruševski, G., Mladenovska, K., et al. (2018). Design and biological response of doxycycline loaded chitosan microparticles for periodontal disease treatment. *Carbohydrate Polymers, 186*, 260–272. https://doi.org/10.1016/j.carbpol.2018.01.043

Ivanoska-Dacikj, A., Makreski, P., Geskovski, N., Karbowniczek, J., Stachewicz, U., Novkovski, N., et al. (2022). Electrospun PEO/rGO scaffolds: the influence of the concentration of rGO on overall properties and cytotoxicity. *International Journal of Molecular Sciences, 23*(2). https://doi.org/10.3390/ijms23020988. Article 2.

Jian, H. J., Anand, A., Lai, J. Y., Unnikrishnan, B., Chang, H. T., Harroun, S. G., et al. (2023). *In situ* hybridization of polymeric curcumin to arginine-derived carbon quantum dots for synergistic treatment of bacterial infections. *ACS Applied Materials & Interfaces, 15*(22), 26457–26471. https://doi.org/10.1021/acsami.3c04316

Jordanov, I., Kolibaba, T. J., Lazar, S., Magovac, E., Bischof, S., & Grunlan, J. C. (2020). Flame suppression of polyamide through combined enzymatic modification and addition of urea to multilayer nanocoating. *Journal of Materials Science, 55*(30), 15056–15067. https://doi.org/10.1007/s10853-020-05074-8

Jordanov, I., Magovac, E., Fahami, A., Lazar, S., Kolibaba, T., Smith, R. J., et al. (2019a). Flame retardant polyester fabric from nitrogen-rich low molecular weight additives within intumescent nanocoating. *Polymer Degradation and Stability, 170*, Article 108998. https://doi.org/10.1016/j.polymdegradstab.2019.108998

Jordanov, I., & Mangovska, B. (2011). Accessibility of mercerized, bioscoured and dried cotton yarns. *IJFTR, 36*(3) [September 2011] http://nopr.niscpr.res.in/handle/123456789/12649.

Jordanov, I., Stevens, D. L., Tarbuk, A., Magovac, E., Bischof, S., & Grunlan, J. C. (2019b). Enzymatic modification of polyamide for improving the conductivity of water-based multilayer nanocoatings. *ACS Omega, 4*(7), 12028–12035. https://doi.org/10.1021/acsomega.9b01052

Karydis-Messinis, A., Moschovas, D., Markou, M., Gkantzou, E., Vasileiadis, A., Tsirka, K., et al. (2023). Development, physicochemical characterization and *in vitro* evaluation of chitosan-fish gelatin-glycerol hydrogel membranes for wound treatment applications. *Carbohydrate Polymer Technologies and Applications, 6*, Article 100338. https://doi.org/10.1016/j.carpta.2023.100338

Kassal, P., Zubak, M., Scheipl, G., Mohr, G. J., Steinberg, M. D., & Murković Steinberg, I. (2017). Smart bandage with wireless connectivity for optical monitoring of pH. *Sensors and Actuators B: Chemical, 246*, 455–460. https://doi.org/10.1016/j.snb.2017.02.095

Khan, F., Liu, P., Xu, F., Ma, Y., & Qiu, Y. (2016). Dye aggregation in layer-by-layer dyeing of cotton fabrics. *RSC Advances, 6*(24), 20286–20293. https://doi.org/10.1039/C5RA27019G

Kiti, K., Thanomsilp, C., & Suwantong, O. (2022). The potential use of colorimetric pH sensor from Clitoria ternatea flower for indicating bacterial infection in wound dressing application. *Microchemical Journal, 177*, Article 107277. https://doi.org/10.1016/j.microc.2022.107277

Li, Y. J., Wei, S. C., Chu, H. W., Jian, H. J., Anand, A., Nain, A., et al. (2022). Poly-quercetin-based nanoVelcro as a multifunctional wound dressing for effective treatment of chronic wound infections. *Chemical Engineering Journal, 437*, Article 135315. https://doi.org/10.1016/j.cej.2022.135315

Magovac, E., Jordanov, I., Grunlan, J. C., & Bischof, S. (2020). Environmentally-benign phytic acid-based multilayer coating for flame retardant cotton. *Materials, 13*(23). https://doi.org/10.3390/ma13235492. Article 23.

Magovac, E., Vončina, B., Budimir, A., Jordanov, I., Grunlan, J. C., & Bischof, S. (2021). Environmentally benign phytic acid-based nanocoating for multifunctional flame-retardant/antibacterial cotton. *Fibers, 9*(11). https://doi.org/10.3390/fib9110069. Article 11.

Magovac, E., Vončina, B., Jordanov, I., Grunlan, J. C., & Bischof, S. (2022a). Layer-by-layer deposition: A promising environmentally benign flame-retardant treatment for cotton, polyester, polyamide and blended textiles. *Materials, 15*(2), 432. https://doi.org/10.3390/ma15020432

Magovac, E., Vončina, B., Jordanov, I., Grunlan, J. C., & Bischof, S. (2022b). Layer-by-layer deposition: A promising environmentally benign flame-retardant treatment for cotton, polyester, polyamide and blended textiles. *Materials, 15*(2). https://doi.org/10.3390/ma15020432. Article 2.

Mariani, F., Serafini, M., Gualandi, I., Arcangeli, D., Decataldo, F., Possanzini, L., et al. (2021). Advanced wound dressing for real-time pH monitoring. *ACS Sensors, 6*(6), 2366–2377. https://doi.org/10.1021/acssensors.1c00552

Marković, D., Petkovska, J., Mladenovic, N., Radoičić, M., Rodriguez-Melendez, D., Ilic-Tomic, T., et al. (2023). Antimicrobial and UV protective chitosan/lignin multilayer nanocoating with immobilized silver nanoparticles. *Journal of Applied Polymer Science, 140*(19), e53823. https://doi.org/10.1002/app.53823

Mary, S. K., Koshy, R. R., Arunima, R., Thomas, S., & Pothen, L. A. (2022). A review of recent advances in starch-based materials: Bionanocomposites, pH sensitive films, aerogels and carbon dots. *Carbohydrate Polymer Technologies and Applications, 3*, Article 100190. https://doi.org/10.1016/j.carpta.2022.100190

Nischwitz, S. P., Bernardelli de Mattos, I., Hofmann, E., Groeber-Becker, F., Funk, M., Mohr, G. J., et al. (2019). Continuous pH monitoring in wounds using a composite indicator dressing—A feasibility study. *Burns : Journal of the International Society for Burn Injuries, 45*(6), 1336–1341. https://doi.org/10.1016/j.burns.2019.02.021

Pakolpakçıl, A., Osman, B., Göktalay, G., Özer, E. T., Şahan, Y., Becerir, B., et al. (2021). Design and *in vivo* evaluation of alginate-based pH-sensing electrospun wound

dressing containing anthocyanins. *Journal of Polymer Research, 28*(2), 50. https://doi.org/10.1007/s10965-020-02400-1

Pal, A., Goswami, D., Cuellar, H. E., Castro, B., Kuang, S., & Martinez, R. V. (2018). Early detection and monitoring of chronic wounds using low-cost, omniphobic paper-based smart bandages. *Biosensors and Bioelectronics, 117*, 696–705. https://doi.org/10.1016/j.bios.2018.06.060

Pang, Q., Yang, F., Jiang, Z., Wu, K., Hou, R., & Zhu, Y. (2023). Smart wound dressing for advanced wound management: Real-time monitoring and on-demand treatment. *Materials & Design, 229*, Article 111917. https://doi.org/10.1016/j.matdes.2023.111917

Petkovska, J., Mladenovic, N., Marković, D., Radoičić, M., Chiang, H. C., Palen, B., et al. (2023). Environmentally benign few-bilayer intumescent nanocoating for flame retardant enzyme/plasma modified polyester fabric. *Polymer Degradation and Stability, 214*, Article 110406. https://doi.org/10.1016/j.polymdegradstab.2023.110406

Petkovska, J., Mladenovic, N., Marković, D., Radoičić, M., Vest, N. A., Palen, B., et al. (2022). Flame-retardant, antimicrobial, and UV-protective lignin-based multilayer nanocoating. *ACS Applied Polymer Materials, 4*(6), 4528–4537. https://doi.org/10.1021/acsapm.2c00520

Rahimi, R., Brener, U., Chittiboyina, S., Soleimani, T., Detwiler, D. A., Lelièvre, S. A., et al. (2018). Laser-enabled fabrication of flexible and transparent pH sensor with near-field communication for *in-situ* monitoring of wound infection. *Sensors and Actuators B: Chemical, 267*, 198–207. https://doi.org/10.1016/j.snb.2018.04.004

Rahimi, R., Ochoa, M., Parupudi, T., Zhao, X., Yazdi, I. K., Dokmeci, M. R., et al. (2016). A low-cost flexible pH sensor array for wound assessment. *Sensors and Actuators B: Chemical, 229*, 609–617. https://doi.org/10.1016/j.snb.2015.12.082

Rani Raju, N., Silina, E., Stupin, V., Manturova, N., Chidambaram, S. B., & Achar, R. R (2022). Multifunctional and smart wound dressings-a review on recent research advancements in skin regenerative medicine. *Pharmaceutics, 14*(8), 1574. https://doi.org/10.3390/pharmaceutics14081574

Saxena, S., & Raja, A. S. M. (2014). Natural dyes: Sources, chemistry, application and sustainability issues. S. S. Muthu (Ed.). *Roadmap to sustainable textiles and clothing: Eco-friendly raw materials, technologies, and processing methods* (pp. 37–80). Springer. https://doi.org/10.1007/978-981-287-065-0_2.

Schaude, C., Fröhlich, E., Meindl, C., Attard, J., Binder, B., & Mohr, G. J. (2017). The development of indicator cotton swabs for the detection of pH in wounds. *Sensors, 17* (6). https://doi.org/10.3390/s17061365. Article 6.

Singh, B., Singh, J., & Rajneesh. (2021). Application of tragacanth gum and alginate in hydrogel wound dressing's formation using gamma radiation. *Carbohydrate Polymer Technologies and Applications, 2*, Article 100058. https://doi.org/10.1016/j.carpta.2021.100058

Sridhar, V., & Takahata, K. (2009). A hydrogel-based passive wireless sensor using a flex-circuit inductive transducer. *Sensors and Actuators A: Physical, 155*(1), 58–65. https://doi.org/10.1016/j.sna.2009.08.010

Sutar, T., Bangde, P., Dandekar, P., & Adivarekar, R. (2021). Herbal hemostatic biopolymeric dressings of alginate/pectin coated with Croton oblongifolius extract. *Carbohydrate Polymer Technologies and Applications, 2*, Article 100025. https://doi.org/10.1016/j.carpta.2020.100025

Uğur, Ş. S., & Sarıışık, M. (2011). Electrostatic self-assembly dyeing of cotton fabrics. *Coloration Technology, 127*(6), 372–375. https://doi.org/10.1111/j.1478-4408.2011.00328.x

Yadav, M., Kaushik, B., Rao, G. K., Srivastava, C. M., & Vaya, D. (2023a). Advances and challenges in the use of chitosan and its derivatives in biomedical fields: A review. *Carbohydrate Polymer Technologies and Applications, 5*, Article 100323. https://doi.org/10.1016/j.carpta.2023.100323

Yadav, S., Tiwari, K. S., Gupta, C., Tiwari, M. K., Khan, A., & Sonkar, S. P. (2023b). A brief review on natural dyes, pigments: Recent advances and future perspectives. *Results in Chemistry, 5*, Article 100733. https://doi.org/10.1016/j.rechem.2022.100733

Yan, D., Li, Y., Liu, Y., Li, N., Zhang, X., & Yan, C. (2021). Antimicrobial properties of chitosan and chitosan derivatives in the treatment of enteric infections. *Molecules, 26* (23). https://doi.org/10.3390/molecules26237136. Article 23.

Yuan, Y., Fan, Q., Xu, X., Wang, O., Zhao, L., & Zhao, L. (2023). Nanocarriers based on polysaccharides for improving the stability and bioavailability of Anthocyanins: A review. *Carbohydrate Polymer Technologies and Applications, 6*, Article 100346. https://doi.org/10.1016/j.carpta.2023.100346